CLM - P 547

CLM - P 547

UKAEA

Preprint

THE KINETIC THEORY OF BEAM INDUCED CURRENTS IN TOROIDAL PLASMAS

J G CORDEY
E M JONES
D F H START
A R CURTIS
I P JONES

CULHAM LABORATORY
Abingdon Oxfordshire

1978

CLM-P 547

THE KINETIC THEORY OF BEAM INDUCED CURRENTS IN TOROIDAL PLASMAS

J G Cordey, E M Jones and D F H Start
Culham Laboratory, Abingdon, Oxon. OX14 3DB, U.K.
(Euratom/UKAEA Fusion Association)

and

A R Curtis and I P Jones
A.E.R.E. Harwell, Didcot, Oxon. OX11 ORA.

ABSTRACT

A Fokker-Planck treatment of the current induced by a beam of fast ions circulating in a toroidal plasma is developed. The electron Fokker-Planck equation is first reduced to an integro-differential equation which is then solved analytically in the limiting cases of: (a) a large plasma Z and (b) a large ratio of the electron thermal velocity v_e to the fast ion velocity v_b. In addition a numerical solution was obtained for the complete range of values of v_e/v_b and for several values of Z. It is found that the resulting net plasma current has a very different functional dependence upon electron temperature than that given by the conventional theoretical treatment in which the electrons are assumed to be Maxwellian. In particular for $v_e > v_b$ and $Z = 1$, which is the limit appropriate to many present Tokamak experiments, the net current is found to be in the opposite direction to the fast ion current. The theory is compared with recent measurements of this current which were made using the Culham Levitron, and agreement is found between theory and experiment.

(Submitted for publication in Nuclear Fusion)

July 1978
ed

1. INTRODUCTION

The possibility of maintaining a steady-state current in a plasma by the injection of fast ions was first proposed by Ohkawa [1] and recent experiments on the Culham Levitron [2] have confirmed the existence of this current. These measurements revealed a substantial discrepancy between the measured current and the theoretically predicted current. In particular, the measured current was found to decrease more sharply with electron temperature than the theoretically predicted current and at higher temperatures the direction of the current appeared to reverse (i.e. it was in the opposite direction to the fast ion current). In this paper it will be shown that the conventional theoretical model in which the electrons are assumed to be Maxwellian is incorrect, and that a more exact Fokker-Planck treatment of the electrons leads to a net current which differs both in its direction and magnitude from the conventional result. The new Fokker-Planck theory is also found to be in much closer agreement with the experimental results than the simpler theory.

The original Ohkawa [1] theory together with other theoretical calculations [2] of this beam induced current have assumed that the electrons can be represented by a displaced Maxwellian distribution. The displacement is then determined by balancing the rate at which momentum is gained by the electrons from Coulomb collisions with the fast ions against the rate of loss to the thermal ions. This analysis has two major shortcomings. First, the velocity dependence of the frictional force between the fast ions and the electrons is, in general, different from that between the thermal ions and the electrons. This leads to the electron distribution being distorted in such a manner that the distribution cannot be represented by a displaced Maxwellian. This distortion of the electron distribution from Maxwellian is similar to that caused by an electric field, which was discussed by Spitzer [3,4] and co-workers in their fundamental papers on the calculation of the resistivity of a plasma.

The second weakness of the Maxwellian electrons model is that electron-electron collisions are not taken into account properly. These two omissions are particularly serious for the present problem, where there is cancellation between the fast ion and electron currents, and thus a precise calculation of the electron distribution is required so that the net current can be accurately determined. In Sections 2 and 3 of this paper the electron distribution function is determined from a Fokker-Planck equation which includes electron-fast ion, electron-thermal ion and electron-electron collisions. The resulting net current is calculated in Section 3 and is found to have a different functional dependence upon the electron temperature from that of the displaced Maxwellian electrons model.

There have been other Fokker-Planck treatments of this problem, Connor et al. [5], Cordey et al. [6] and Fomenko [7] but these authors considered only the limit of the electron thermal velocity v_e being much greater than the fast ion velocity v_b. Also electron-electron collisions were ignored in all of these papers and although this is valid in the limit $v_e >> v_b$ it cannot be justified when the inequality does not hold.

The present paper has the following structure. In Section 2 the electron Fokker-Planck equation is reduced to an integro-differential equation in the velocity variable v. Then, in Section 3, analytic solutions are obtained in the limits of $Z >> 1$ (the Lorentz gas approximation) and $v_e >> v_b$. These solutions are then compared with the numerical solution of the full equation which is given in the final part of Section 3. A comparison of the numerical solution with the results of the Levitron measurements of the beam induced current is made in Section 4.

2. REDUCTION OF THE ELECTRON FOKKER-PLANCK EQUATION

To simplify the Fokker-Planck equation the usual assumption is made that the number density of the fast ions n_b is much smaller than the thermal particle density n. The perturbation of the electron distribution function from Maxwellian is then small so that it can be written in the form:

$$f_e = F_{me} + f'_e \qquad \ldots (1)$$

where F_{me} is the Maxwellian distribution. The electron Fokker-Planck equation, correct to the first order in f'_e may then be written symbolically in the form,

$$C_{eb}(F_{me}, f_b) + C_{ei}(f'_e, F_{mi}) + C_{ee}(f'_e, F_{me}) + C_{ee}(F_{me}, f_e) = 0 \qquad \ldots (2)$$

where C is the linearised collision operator. The reference frame is such that the thermal ions are at rest, and f_b is the fast ion distribution. This distribution may be obtained from a fast ion Fokker-Planck equation in the manner described by Cordey and Core [8] or Callen et al. [9]. Thus for the purposes of this paper the fast ion distribution is assumed to be known and taken in the form:

$$f_b = \Sigma\, a_{nb}(v)\, P_n(\xi) \qquad \ldots (3)$$

where $\xi = v_{||}/v$.

In the Levitron experiments the fast ion slowing down time was an order of magnitude longer than the charge exchange loss time so that the fast ion distribution was essentially monoenergetic. In this case the coefficients $a_{nb}(v)$ become:

$$a_{nb}(v) = \frac{(n+\frac{1}{2})\, K_n\, n_b\, \delta(v - v_b)}{2\pi\, v_b^2} \qquad \ldots (4)$$

where

$$K_n = \int_{-1}^{1} K(\xi)\, P_n(\xi) d\xi \qquad \ldots (5)$$

and $K(\xi)$ is the angular distribution of the fast ions normalised such that $\int_{-1}^{1} K(\xi) d\xi = 1$. From here onwards it is assumed, for simplicity, that the fast ion distribution has the form given by Eqs.(3) - (5). Distributions which are not strongly peaked may be easily handled using a Green's function technique with v_b as the variable of integration.

Since all the distributions are symmetric about the field lines the electron distribution can be expanded without loss of generality as a series Legendre polynomials

$$f'_e = F_{me} \Sigma\, a_n(v)\, P_n(\xi) \; . \qquad \ldots (6)$$

Similarly the Rosenbluth potentials h and g [10] which occur in the collision operator may also be expanded as a series of Legendre polynomials in the form

$$h = \Sigma\, h_n(v)\, P_n(\xi) \quad \text{etc.} \qquad \ldots (7)$$

Substitution of expression (6) into Eq.(2) leads to a set of uncoupled equations for the coefficients $a_n(v)$. Since we are only interested in the current along the field lines, only $a_1(v)$ is required. The equation for $a_1(v)$ is an integro-differential equation which can be expressed in terms of the normalised velocity variable $x = v/v_e$ as

$$a_1'' + P(x)a_1' + Q(x)a_1 = \frac{16}{3\pi^{\frac{1}{2}}\Lambda}\left[xI_3(x) - 1.2x\, I_5(x) - x^4(1-1.2x^2)\right.$$
$$\left.(I_o(x) - I_o(\infty))\right] + R(x) \qquad \ldots (8)$$

with

$$P(x) = -x^{-1} - 2x + 2x^2\, \Phi'/\Lambda \qquad \ldots (9)$$

$$Q(x) = x^{-2} - 2\,(Z + \Phi - 2x^3\Phi')/\Lambda \qquad \ldots (10)$$

$$R(x) = -\frac{B}{\Lambda}\left\{\begin{array}{ll} v_b^{*-2}\,(\frac{6}{5}x^6 - 2x^4) & x < v_b^* \\ (v_b^* + \frac{6}{5}v_b^{*3})x & x > v_b^* \end{array}\right\} \qquad \ldots (11)$$

$$\Lambda = \Phi - x\,\Phi' \qquad \ldots (12)$$

$$\Phi(x) = \mathrm{erf}(x) = \frac{2}{\pi^{\frac{1}{2}}}\int_o^x \exp(-x^2)dx \qquad \ldots (13)$$

$$I_n(x) = \int_o^x a_1(y)e^{-y^2}\, y^n\, dy \qquad \ldots (14)$$

where v_b^* is the normalised beam velocity defined as $v_b^* = v_b/v_e$, n is the plasma density, Z the effective plasma charge, $Z = \Sigma\, n_i\, Z_i^2/n_e$, the dash is the derivative with respect to x and the constant $B = 4\, K_1\, n_b/n$.

Eq.(8) is identical to that of Spitzer and Härm [4] except that the term $R(x)$, which drives the current, is due to the fast ions colliding with the electrons. In the Spitzer problem, where the current is driven by an electric field,

$$R(x) = -2\, A\, x^4/\Lambda\,. \qquad \ldots (15)$$

The integral $I_o(\infty)$ may be determined by taking the first moment of the Fokker-Planck Eq.(2) (this is equivalent to multiplying Eq.(8) by Λe^{-x^2} and integrating). Since electron-electron collisions cannot transfer momentum they do not contribute to this first moment. Only the electron-ion collision

terms contribute, these are the $R(x)$ term and the part of the $Q(x)$ term which is proportional to Z. This gives

$$I_o(\infty) = \frac{B}{2Z}\left[v_b^{*-2} \int_o^{v_b^*} (1.2x^6 - 2x^4)e^{-x^2}\, dx + 0.5(v_b^* + 1.2v_b^{*3})e^{-v_b^{*2}} \right]$$

which after successive integration by parts reduces to

$$I_o(\infty) = 3\pi^{\frac{1}{2}}\, B\, \Lambda(v_b^*)/16Zv_b^{*2} \qquad \ldots (16)$$

Using the above expression for $I_o(\infty)$, Eq.(8) can be rewritten in the form used by Spitzer and Härm [4] for the numerical evaluation of $a_1(x)$, namely,

$$a_1'' + P(x)a_1' + Q(x)a_1 = S_N(x) + R_N(x) \quad , \qquad \ldots (17)$$

where

$$S_N(x) = \frac{16}{3\pi^{\frac{1}{2}}\Lambda}\left[x\, I_3(x) - 1.2x\, I_5(x) - x^4(1-1.2x^2)I_o(x) \right] \quad , \qquad \ldots (18)$$

and $R_N(x)$ now has the form,

$$R_N(x) = -\frac{B}{\Lambda}\left\{ \begin{array}{ll} v_b^{*-2}\,(1.2x^6 - 2x^4) - \dfrac{x^4(1-1.2x^2)\Lambda(v_b^*)}{Zv_b^{*2}} & ;\ x < v_b^* \\ (v_b^* + 1.2v_b^{*3})x - \dfrac{x^4(1-1.2x^2)\Lambda(v_b^*)}{Zv_b^{*2}} & ;\ x > v_b^* \end{array} \right\} \qquad \ldots (19)$$

The boundary conditions for $a_1(x)$ are that it be well-behaved at $x = 0$ and $x = \infty$. Examination of the behaviour of $a_1(x)$ at these boundaries shows that it must approach the series solutions of Eq.(7) at small and large x. These solutions have the following forms:

$$a_1(x) \to -\frac{B}{Z}\left(v_b^{*-2} + \frac{8I_o(\infty)}{3\pi^{\frac{1}{2}}\, B} \right)\left[x^4 + \frac{12x^5}{\pi^{\frac{1}{2}}\, Z} + \ldots \right] \quad \text{as } x \to 0 \qquad \ldots (20)$$

and

$$a_1(x) \to -\frac{1}{(Z+2)}\left[\frac{8\left(I_3(\infty) - 1.2I_5(\infty)\right)}{3\pi^{\frac{1}{2}}} - \frac{B}{2}\,(v_b^* + 1.2\, v_b^{*3}) \right] x + O(x^{-Z-1}) \quad \text{as } x \to \infty \qquad \ldots (21)$$

The small x solution is an asymptotic series, the terms diverging as $(n+2)!(n+5)!\, x^n$. Thus to obtain an accurate boundary condition very small values of x of the order $10^{-3} \sim 10^{-4}$ have to be used.

In the next section analytic solutions of Eq.(17) are derived in the limits of $Z \gg 1$ and $v_b^* \ll 1$. In the last part of Section 3, Eq. (17) is solved numerically for a range of values of Z from 1 to 16 with values of v_b^* from 0.1 to 10.

3. SOLUTION OF THE INTEGRO-DIFFERENTIAL EQUATION

(a) Lorentz Gas Limit, $Z \gg 1$

In the Lorentz gas limit electron-electron collisions are neglected and only electron-ion collisions are taken into account. The solution of Eq.(17) in this limit ($Z \to \infty$) is:

$$a_1(x) = \frac{B}{2Z} \begin{cases} v_b^{*-2}(1.2x^6 - 2x^4) & ; \quad x < v_b^* \\ (v_b^* + 1.2\, V_b^{*3})\, x & ; \quad x > v_b^* \end{cases} \quad \ldots (22)$$

From this solution the integrals $I_3(\infty)$ and $I_5(\infty)$ can be evaluated.

The electron current is given by $j_e = -e \int v_{||} f_e' \, d^3v$ and may be written in terms of $I_3(\infty)$ in the following form

$$j_e = -\frac{4e}{3\pi^{\frac{1}{2}}} v_e \, n \, I_3(\infty)$$

The expression for the total current (i.e. the fast ion current plus electron current) is:

$$j = e K_1 \left(n_b v_b - \frac{4}{3} \frac{v_e}{\pi^{\frac{1}{2}} K_1} n I_3(\infty) \right) \quad \ldots (23)$$

Eq.(23) may be expressed more conveniently by normalising with respect to the fast ion current and thus we define

$$F = j/n_b e v_b K_1 = 1 - \frac{16\, I_3(\infty)}{3\pi^{\frac{1}{2}} v_b^* B} \quad \ldots (24)$$

where F is the ratio of the net current to the fast ion current. Substituting expression (22) for $a_1(x)$ in Eq.(14) to obtain $I_3(\infty)$ gives

$$F = 1 - \frac{16\, v_b^{*-3}}{5\, \pi^{\frac{1}{2}} Z} \left\{ 7 - e^{-v_b^{*2}} \left(7 + 7v_b^{*2} + \frac{7}{2} v_b^{*4} + \frac{17}{3} v_b^{*6} - 4v_b^{*8}\right) \right\} \quad \ldots (25)$$

$$- \frac{4}{5\pi^{\frac{1}{2}} Z} \left\{ \left(\frac{68}{3} v_b^{*3} - 16\, v_b^{*5} + 2.5\, v_b^* \right) e^{-v_b^{*2}} + \left(2.5 + 3\, v_b^{*2}\right) \frac{\pi^{\frac{1}{2}}}{2} \operatorname{erfc}(v_b^*) \right\}$$

The above expression for F in the Lorentz gas approximation is given by the dashed curves in Figs.1-3 as a function of v_b^{*-2} ($\equiv v_e^2/v_b^2$) for $Z = 1,2,4$. (F is plotted as a function of v_b^{*-2} ($\equiv T_e/\varepsilon_b$) since the experimental results in Section 4 are a function of T_e.) An interesting feature on the $Z = 1$ curve is that for large v_b^{*-2} the net current has the opposite sign to the fast ion current. This means that the electron current actually exceeds the fast ion current. Although, of course, the analysis of this section is not strictly valid for the $Z = 1$ case it will be seen later that even when

electron-electron collisions are taken into account, the current is still negative over a wide range of v_b^{*-2}.

Using the series expansion of the complementary error function Eq.(25), in the limit of small v_b^*, reduces to

$$F \to 1 - \frac{1}{Z} - 1.2\,\frac{v_b^{*2}}{Z} \quad \text{as} \quad v_b^* \to 0 \,. \qquad \ldots (26)$$

This form is identical to that of Fomenko [7] who assumed that the Lorentz gas approximation was valid without justification and took $v_b^* << 1$ from the beginning. In the next section the full Eq.(17) (including electron-electron collisions) is solved in the limit $v_b^* << 1$ and it will be shown that the exact F does indeed tend to the Lorentz limit as $v_b^* \to 0$.

b) High Electron Temperature Limit $v_b^*(= v_b/v_e) << 1$

This limit is important because most of the present neutral injection experiments on Tokamaks satisfy the above condition ($v_b^* << 1$). The objective here is to obtain the net current correct to order v_b^{*3}, and the procedure is as follows. A particular integral of Eq.(17) is obtained correct to order v_b^{*3}. This integral has a discontinuity at $x = v_b^*$ and to make the solution continuous a prescribed amount of the general solution must be added to it. The general solutions of Eq.(17) are both very rapidly varying exponentials and have the effect of replacing the discontinuity in the particular integral by a very narrow transition region in which the solution changes continuously but sharply between the two values of the particular integral on either side of the discontinuity. Indeed the transition region is so narrow that the solution in that region makes no contribution to the net current.

The particular integral of Eq.(17) that was used has the following form

$$a_1(x) = \left\{ \begin{array}{ll} -B\,x^4/Z\,v_b^{*2} & ;\quad x < v_b^* \\ B\,(v_b^* + 1.2\,v_b^{*3})x/2Z & ;\quad x > v_b^* \end{array} \right\} \qquad \ldots (27)$$

In the above equation, the expression for $x < v_b^*$ is just the first term of the small x series solution of Eq.(17) (given by Eq.(20)). The solution for $x > v_b^*$ is the Lorentz solution in this region. Substituting expression (27) for $a_1(x)$ into Eq.(17) it can be shown that this solution is indeed correct to order v_b^{*3}.

The part of the general solution of Eq.(17) which has to be added to Eq.(27) to make $a_1(x)$ continuous is now evaluated. Eq.(17) is expanded in the vicinity of the transition region $x = v_b^*$ by making the transformation of variable $y = x - v_b^*$. Neglecting terms of order y and keeping only the leading terms in v_b^*, the homogeneous part of Eq.(17) becomes

$$a_1'' - \frac{1.5\pi^{\frac{1}{2}}}{v_b^{*3}} a_1 = 0 \qquad \ldots (28)$$

where the dash is now differentiation with respect to y.

The general solution of Eq.(28) is

$$a_1(y) = C \exp(\beta y/v_b^{*3/2}) + D \exp(-\beta y/v_b^{*3/2}) \qquad \ldots (29)$$

where C and D are arbitrary constants and $\beta = (1.5\ \pi^{\frac{1}{2}})^{\frac{1}{2}}$. The above solutions are both strongly varying with a scale length of the order of $v_b^{*3/2}$. Since the complete solution must be well behaved at both $x = 0$ (i.e. $y = -v_b^*$ and $x = \infty$ $(y = \infty)$, the value of C must be zero for $x > v_b^*$ $(y > 0)$ and the value of D must be zero for $x < v_b^*$ $(y < 0)$. That is, only the solutions which decay exponentially away from the transition region are physically possible. The remaining constants C in the region $y < 0$ and D in the region $y > 0$ can be determined by ensuring that a_1 and a_1' are continuous at $y = 0$. As a result the complete solution for small v_b^* is

$$a_1(x) = \frac{B}{2Z} \begin{cases} -2x^4/v_b^{*2} + 1.5\ v_b^{*2} \exp\{\beta(x - v_b^*)/v_b^{*3/2}\} & ;\ x < v_b^* \\ (v_b^* + 1.2\ v_b^{*3})x - 1.5\ v_b^{*2} \exp\{-\beta(x - v_b^*)/v_b^{*3/2}\} & ;\ x > v_b^* \end{cases} \qquad \ldots (30)$$

The integral $I_3(\infty)$ may be obtained from the above expression by quadrature and then using Eq. (24) we find that the ratio of the net current to the beam current correct to order v_b^{*2} is

$$F = 1 - \frac{1}{Z} - 1.2\ \frac{v_b^{*2}}{Z} \quad . \qquad \ldots (31)$$

Interestingly this is the same expression as that given by Eq.(26) for the Lorentz gas case in the limit $v_b^* \to 0$. Thus at small v_b^* (high electron temperatures) the solution of the full equation approaches the Lorentz gas result.

c) Numerical Solution of Full Equation

The numerical solution of Eq.(17) is not completely straightforward. The main difficulty, as Spitzer et al. [3] showed, is that the complementary function solutions are rapidly increasing and decreasing exponentials and so direct numerical integration of Eq.(17) fails. The integration of Eq.(17) is in fact unstable for both increasing and decreasing x; i.e. a small deviation from the correct solution increases so rapidly in the course of the integration that any trace of the correct solution soon disappears. This behaviour is due to the singular nature of $Q(x)$ which varies as $1/x^3$ for small x. Two independent numerical techniques were developed to overcome this numerical instability problem. The first method was identical to the variation of parameters technique used by Spitzer et al. [3]. The second method which is described in the Appendix was a two point boundary value technique. This second method was found to be considerably more flexible than the first technique in that non-integer values of Z could be handled.

The results from both techniques agreed to within 0.5% and the values of $I_3(\infty)$ given in Table A1 were obtained using the two point boundary value technique and are accurate to four decimal places. The flexibility of the two point boundary value technique also enables us to solve the Spitzer resistivity problem for non-integer Z. In Table A2, values of γ_E, the ratio of the conductivity to the Lorentz conductivity, are given for a range of Z values from 1 to 16.

Returning to the beam induced current problem, the ratio of the net current to the fast ion current F, is evaluated using $I_3(\infty)$, and is given in Table A3. In Figs 1 - 3 the parameter F (continuous curves) is shown as a function of $v_b^{*-2} (= v_e^2/v_b^2)$ for $Z = 1,2,4$. These curves may be compared with those for the Lorentz gas approximation and also with the corresponding curves for the conventional displaced Maxwellian theory which is described in reference [2].

Points of interest in Figs.1-3 are first that the net current is in the opposite direction to the beam current for $Z = 1$ when $v_b^* < 1.35$ and in the

opposite direction to that of the displaced Maxwellian approximation. Secondly, there is, as expected, a significant difference between the Lorentz approximation curve and the exact curve for Z = 1. This indicates the importance of electron-electron collisions for low Z plasmas. The effect of course becomes less significant at larger values of Z.

4. COMPARISON WITH CULHAM LEVITRON EXPERIMENTS

In the Levitron experiments [2] a modulated beam of fast protons was injected into a hydrogen plasma and the net circulating current was detected through the voltage induced in a pick-up coil which looped the plasma in the poloidal direction. The signal due to current flowing parallel to the magnetic field lines was measured as a function of the plasma electron temperature and the results obtained are taken from reference [2] and shown in Fig.4. The error bars represent the statistical errors. Systematic errors in the absolute magnitude of the points due to uncertainties in the absolute density and beam intensity measurements are estimated to be less than 15%. The solid curves are theoretical predictions evaluated for the average beam energy of 8.5 keV and for uniform plasma parameters. The values of F, the ratio of the net current to the fast ion current for these curves are shown on the right of Fig.4. In the range of interest the displaced Maxwellian theory underestimates the reverse electron current by a factor of two. On the other hand, the Lorentz gas approximation predicts too large an electron current by a similar factor. Much better agreement with experiment is achieved by the Fokker-Planck theory of Section 3 which includes electron-electron collisions. The dashed curve in Fig.4 shows the effect of incorporating the measured plasma density and temperature profiles in the full Fokker-Planck treatment.

The above theoretical predictions take no account of the presence of trapped electrons which serve to inhibit the reverse electron current, or of the dependence of the Coulomb logarithm ($\ell n \Lambda$) on the fast ion velocity. The effect of the trapped particles can be estimated using the expression of Hinton and Hazeltine [11] for the analogous case of an electric field driven

current. For the Levitron, the trapped particles are estimated to reduce the predicted electron current by 7% at $\overline{T}_e$ = 1 eV and 13% at 4.7eV. Corrections to the energy loss rates due to the dependence of $\ell n\Lambda$ on the test particle velocity have been given by Itikawa and Aono [12] and these indicate that the electron current should be increased by 20% at $\overline{T}_e$ = 1 eV and reduced by 3% at $\overline{T}_e$ = 4.7 eV.

ACKNOWLEDGEMENTS

It is a pleasure to acknowledge useful discussion on the numerical solution of Eq.(8) with Nancy Nichols, Jeremy Field and Bill Morton.

REFERENCES

[1] Ohkawa, T. Nucl. Fusion 10 185 (1970).

[2] Start, D F H., Collins, P R., Jones, E M., Riviere, A C., and Sweetman, D R. Phys. Rev. Lett. 40 1497 (1978).

[3] Cohen, R S., Spitzer, L and Routly, P. Phys. Rev. 80 230 (1950).

[4] Spitzer, L., and Härm, R. Phys. Rev. 89 977 (1953).

[5] Connor, J W., and Cordey, J G. Nuclear Fusion 14 185 (1974).

[6] Cordey, J G., and Haas, F A. Plasma Physics and Controlled Nuclear Fusion Research (Proc. 6th Int. Conf. Berchesgaden 1976) 2, IAEA Vienna 423 (1977).

[7] Fomenko, V V., Nuclear Fusion 15 1091 (1975).

[8] Cordey, J G and Core, W G F., Phys. Fluids 17 (1974) 1626 and Nuclear Fusion 15 755 (1975).

[9] Callen, J D., Colchin, R J., Fowler, R H., McAlees, D G and Rome, J A. in Plasma Physics and Controlled Nuclear Fusion Research (Proc. 5th Int. Conf. Tokyo 1974) 1, IAEA Vienna 645 (1975).

[10] Rosenbluth, M N., MacDonald, R M and Judd, D L., Phys. Rev. 107 1 (1957).

[11] Hinton, F L., and Hazeltine, R D., Rev. Mod. Phys. 48 239 (1976).

[12] Itakawa, Y and Aono, O., Phys. Fluids 9 1259 (1966).

[13] Lentini, M and Pereyra, V. Siam J. Num. Anal. 14 pp.91-111 (1977).

APPENDIX

NUMERICAL SOLUTION AS A TWO-POINT BOUNDARY VALUE PROBLEM

The differential equation defined by Eq(8) to Eq(14) was solved as a two-point boundary value problem on a range $a \leqslant x \leqslant b$, where a was small and $4 \leqslant b \leqslant 5$, by the method of Lentini and Pereyra [13] using their algorithm PASVAR which (in the version PASVA3) is in the Harwell Subroutine Library under the name DD04AD. In the case of the discontinuous forcing function Eq(11), the discontinuity at $x = v_b$ was smoothed by replacing $R(x)$ with,

$$R(x) = \frac{1}{2}\left[R_1(x) + R_2(x) + (R_2(x) - R_1(x)) \tanh \left(\frac{x-v_b^*}{s}\right) \right] \qquad \ldots (A1)$$

where $R_1(x)$, $R_2(x)$ are the forms for $x < v_b^*$ and $x > v_b^*$ respectively, and s is a small number.

The initial mesh required by DD04AD was generated with: a) constant spacing 0.1 in $\log_{10}(x)$ over the range $a < x < 1$; b) constant spacing 0.2 in x over $1 < x < b$; c) in addition, eleven equally spaced points centred on $x = v_b$, with spacing $\frac{1}{2}S$. A limit of $N < 300$ was set on the number, N, of points in the final mesh generated by the program. The error tolerance τ was taken as a limit on the estimate of absolute error in each solution component at each point on the final mesh.

The problem must be specified to DD04AD as a first-order system

$$\frac{dy_i}{dx} = f_i(x, y_1, y_2, \ldots, y_m), \qquad i = 1 \text{ to } m \qquad \ldots (A2)$$

with boundary conditions

$$0 = g_i(y_1(a), \ldots, y_m(a), y_1(b), \ldots, y_m(b)), \qquad i = 1 \text{ to } m\,. \qquad \ldots (A3)$$

For our problem m = 5, and the y_m are defined as

$$\left.\begin{aligned} y_1 &= a_1(x) \\ y_2 &= a_1'(x) \\ y_3 &= I_o(x) \\ y_4 &= I_3(x) \\ y_5 &= 1.2\, I_5(x) - I_3(x) \end{aligned}\right\} \qquad \ldots (A4)$$

so that the functions (A2) are

$$\left.\begin{aligned} f_1 &= y_2 \\ f_2 &= R(x) - P(x)\, y_2 - Q(x)\, y_1 + S(x) \\ f_3 &= e^{-x^2}\, y_1 \\ f_4 &= x^3\, f_3 \\ f_5 &= (1.2x^2 - 1)\, f_4 \end{aligned}\right\} \qquad \text{(A5)}$$

where

$$S(x) = \frac{-16}{3\pi^{\frac{1}{2}}\Lambda(x)} \left[x y_5(x) + x^4(1.2x^2-1)(I_o(\infty) - y_3(x)) \right]$$

and

$$I_o(\infty) = -\frac{1}{2Z} \int_0^\infty R(x)\, \Lambda(x)\, e^{-x^2} dx$$

$$= \left\{ \begin{array}{ll} \dfrac{3\pi^{\frac{1}{2}}\, B}{16Z\, v_b^{*2}}\, \Lambda(v_b^*), & \text{for (11)} \\ \dfrac{3\pi^{\frac{1}{2}} A}{8Z}, & \text{for (15)} \end{array} \right\} \qquad \ldots \text{(A6)}$$

It was essential to choose the boundary conditions with some care since a poor choice results in the introduction of complementary functions which decrease inward from the boundary and cause the computed solution to differ considerably from the true solution near the end of the range.

From Eq.(20) the dependence of $a_1(x)$, for small x, is $a_1(x) = 0(x^4)$ (and similar for the Spitzer $R(x)$), so four of the conditions (A3) were chosen as homogeneous ones derived from this fact, and have form:

$$\left.\begin{aligned} 0 &= y_2(a) - 4y_1(a)/a \\ 0 &= y_1(a) - 8y_4(a)/a^4 \\ 0 &= y_4(a) + y_5(a) \\ 0 &= y_3(a) - a y_1(a)/5 \end{aligned}\right\} \qquad \ldots \text{(A7)}$$

It was then necessary to choose a condition at $x = b$, to control the complementary function which increases with x. Assuming that $a_1(x) \sim c\, x^d$ for large x, the terms of Eq(8) are approximately (ignoring terms of order e^{-x^2})

$$
\left.
\begin{aligned}
& a_1'' \sim c\, d(d-1)\, x^{d-2} \\
& P(x)\ a_1' \sim -2\, cd\, x^{d}\left(1 + \tfrac{1}{2}x^{-2}\right) \\
& Q(x)\ a_1 \sim -c\, x^{d}\left(2(Z+1) - x^{-2}\right) \\
& S(x) \sim -\frac{16x}{3\pi^{\frac{1}{2}}}\, y_5(\infty) \\
& R(x) = \begin{cases} -Bv_b^{*}\left(1 + 1.2\, v_b^{*2}\right)x, & \text{for Eq(11)} \\ -2Ax^{4}, & \text{for Eq(15)} \end{cases}
\end{aligned}
\right\} \qquad \ldots \text{(A8)}
$$

For Eq(11) we must clearly take d = 1, so that a_1'' arises only from relatively small terms of order (d - 2), and so is itself of relative order x^{-4}. Therefore we should get a good approximation to a suitable boundary condition by ignoring a_1'' taking the condition as

$$Q(b)\, y_1(b) + P(b) y_2(b) + \frac{16b}{3\pi^{\frac{1}{2}}}\, y_5(b) - R(b) = 0\ . \qquad \ldots \text{(A9)}$$

This worked adequately,but was not ideal because (with b in the range 4 to 5) the neglected terms were still fairly important.

For the Spitzer problem Eq(15) we clearly have d = 4, and a_1'' is now of relative order x^{-2} rather than x^{-4}. However, the same condition (A9) was used, and again it worked adequately.

Most of the runs were carried out with the following parameter values:

$$a = 10^{-4}$$

$$b = 5$$

$$\tau = 10^{-5}$$

$$s = 2.10^{-3}$$

Spot tests with larger values of a (up to 10^{-3}), smaller values of b (down to 4), or larger values of s (up to 0.01) confirmed the reliability of computed values of $I_3(\infty)$ and their insensitivity to these parameters. Checking $y_3(b)$ against Eq (A6) also gave valuable confidence in the results. We also used smaller values of τ in some tests, to confirm that a value of 10^{-5} was adequate. In some cases, especially at small v_b^{*} where the effect of the discontinuity is relatively severe, it was necessary to relax the parameter values, within the ranges quoted, in order to obtain a successful solution within the bound on mesh size N.

These numerical experiments confirmed that the values of $I_3(\infty)$ quoted in Tables A1 and A2 are accurate to within one or two units in the last place quoted. The corresponding values of F (the ratio of the net current to the fast ion current) are given in Table A3.

Table A1: Values of $I_3(\infty)/B$ for R(x) given by Eq (11)

Z =	1.0	1.1	1.2	1.5	2.0	4.0	8.0	16.0
v_b^*								
0.1	0.03363	0.03058	0.02803	0.02242	0.01682	0.00841	0.004204	0.002102
0.2	0.06951	0.06322	0.05797	0.04640	0.03481	0.01741	0.008706	0.004353
0.3	0.10905	0.09930	0.09114	0.07312	0.05497	0.02756	0.013786	0.006894
0.5	0.19823	0.18142	0.16727	0.13559	0.10310	0.05257	0.026492	0.013282
0.7	0.29063	0.26773	0.24828	0.20418	0.15791	0.08312	0.042659	0.021580
0.8	0.33291	0.30766	0.28615	0.23706	0.18499	0.09916	0.051515	0.026238
1.0	0.40056	0.37238	0.34821	0.29244	0.23213	0.12902	0.068824	0.035636
1.3	0.44641	0.41798	0.39343	0.33601	0.27244	0.15874	0.087915	0.046711
1.5	0.44085	0.41429	0.39126	0.33703	0.27629	0.16504	0.093321	0.050333
2.0	0.35410	0.33468	0.31774	0.27742	0.23139	0.14385	0.084154	0.046553
3.0	0.17836	0.16903	0.16087	0.14136	0.11887	0.07535	0.044822	0.025108
3.8	0.11143	0.10561	0.10052	0.08834	0.07414	0.04712	0.028046	0.015716
6.0	0.04470	0.04236	0.04032	0.03544	0.02981	0.01890	0.011250	0.006304
10.0	0.01609	0.01525	0.01452	0.01276	0.01073	0.00681	0.004050	0.002266

Table A2: Values of $I_3(\infty)/A$ for the Spitzer resistivity problem and the ratio of the conductivity to the Lorentz gas conductivity γ_E as a function of Z

Z	$I_3(\infty)/A$	γ_E
1.0	1.74578	0.5819
1.1	1.62507	0.5959
1.2	1.52184	0.6087
1.4	1.35392	0.6318
1.6	1.22252	0.6520
1.8	1.11642	0.6699
2.0	1.02865	0.6858
2.5	0.86288	0.7191
3.0	0.74556	0.7456
4.0	0.58900	0.7853
5.0	0.48838	0.8140
6.0	0.41784	0.8357
8.0	0.32495	0.8665
10.0	0.26625	0.8875
12.0	0.22568	0.9027
14.0	0.19592	0.9143
16.0	0.17313	0.9234

Table A3: The ratio of the total current to the fast ion current $F = 1 - 16I_3(\infty)/(3\pi^{\frac{1}{2}}v_b^*B)$

$Z =$	1.0	1.1	1.2	1.5	2.0	4.0	8.0	16.0
v_b^*								
0.1	-0.01193	0.07984	0.15657	0.32538	0.49388	0.74694	0.873501	0.936751
0.2	-0.04578	0.04885	0.12784	0.30191	0.47628	0.73807	0.869018	0.934509
0.3	-0.09378	0.00402	0.08586	0.26660	0.44865	0.72357	0.861726	0.930853
0.5	-0.19295	-0.09179	-0.00663	0.18402	0.37954	0.68363	0.840571	0.920069
0.7	-0.24930	-0.15086	-0.06725	0.12231	0.32121	0.64270	0.816627	0.907236
0.8	-0.25216	-0.15719	-0.07629	0.10836	0.30420	0.62703	0.806239	0.901312
1.0	-0.20529	-0.12050	-0.04777	0.12004	0.30152	0.61178	0.792908	0.892771
1.3	-0.03327	0.03253	0.08936	0.22226	0.36940	0.63258	0.796510	0.891882
1.5	0.11565	0.16893	0.21513	0.32392	0.44576	0.66893	0.812797	0.899032
2.0	0.46725	0.49647	0.52196	0.58262	0.65187	0.78358	0.873390	0.929961
3.0	0.82110	0.83046	0.83865	0.85822	0.88077	0.92442	0.955043	0.974817
3.8	0.91176	0.91637	0.92040	0.93005	0.94129	0.96269	0.977792	0.989555
6.0	0.97758	0.97876	0.97978	0.98223	0.98505	0.99052	0.994358	0.996839
10.0	0.99516	0.99541	0.99563	0.99616	0.99677	0.99795	0.998781	0.999318

Figure Captions

Fig.1 The ratio of the net current to the fast ion current F, as a function of v_e^2/v_b^2 ($\equiv v_b^{*-2}$) for an effective charge Z = 1. The continuous curve is the numerical solution of the full Fokker-Planck equation, the dashed curve the Lorentz approximation and the dot-dashed curve the displaced Maxwellian approximation [2] ($F = 1 - 4\, I_o(\infty)/B\, v_b^*$).

Fig.2 The ratio of the net current to the fast ion current F, as a function of $v_e^2/v_b^2 (\equiv v_b^{*-2})$ for Z = 2.

Fig.3 The ratio of the net current to the fast ion current F, as a function of $v_e^2/v_b^2 (\equiv v_b^{*-2})$ for Z = 4.

Fig.4 Comparison of the theoretical temperature dependence of the net current with the Levitron experimental results (reference 2). The full curves show the predictions of the displaced Maxwellian approximation, the full Fokker-Planck theory and the Lorentz approximation for uniform plasma parameters. The dashed curve shows the effect of averaging the parameter F over the experimental profiles in the case of the full Fokker-Planck theory.

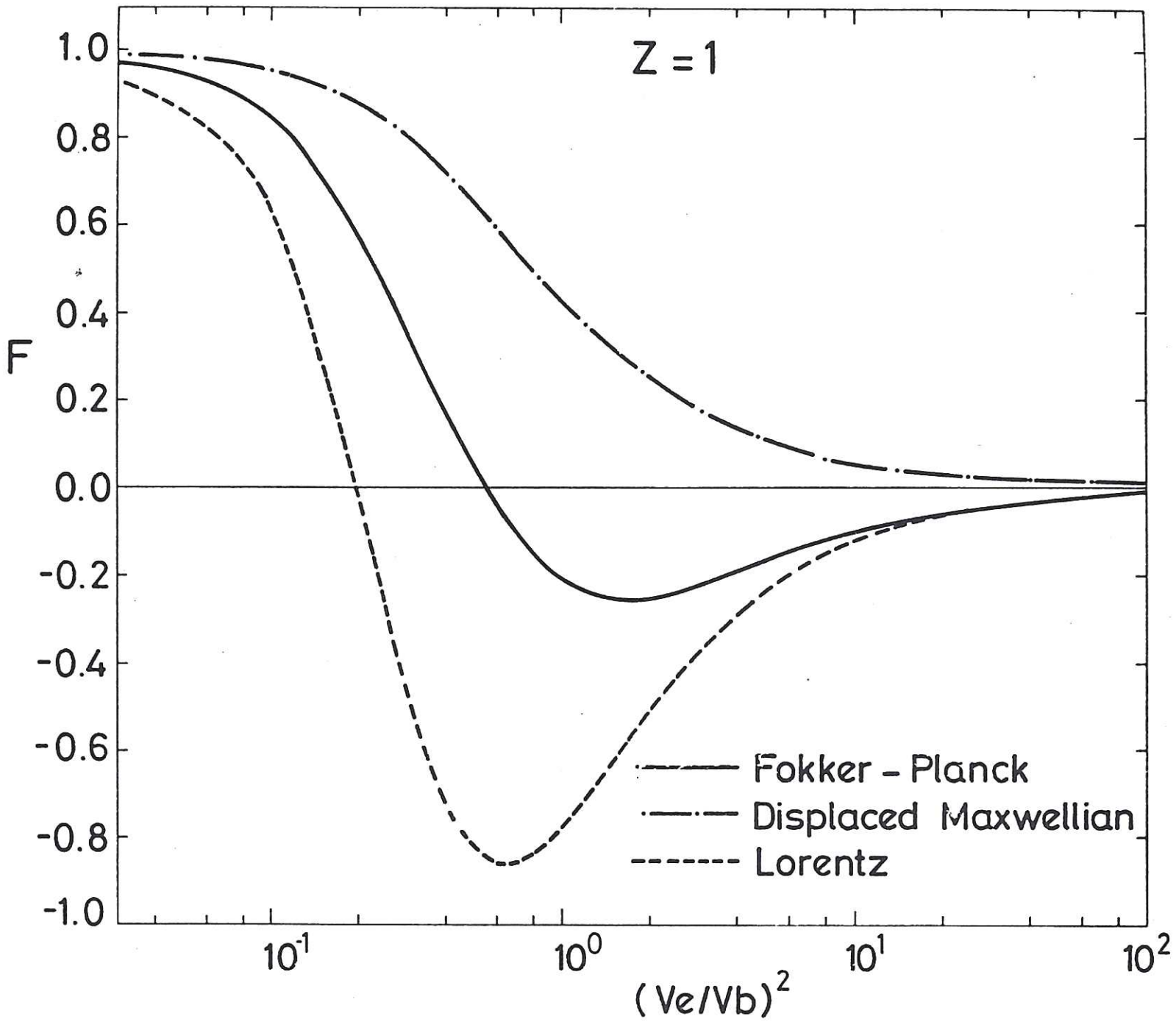
Z = 1
F
1.0
0.8
0.6
0.4
0.2
0.0
-0.2
-0.4
-0.6
-0.8
-1.0
10^{-1}
10^{0}
10^{1}
10^{2}
$(Ve/Vb)^2$
Fokker - Planck
Displaced Maxwellian
Lorentz

FIG 1

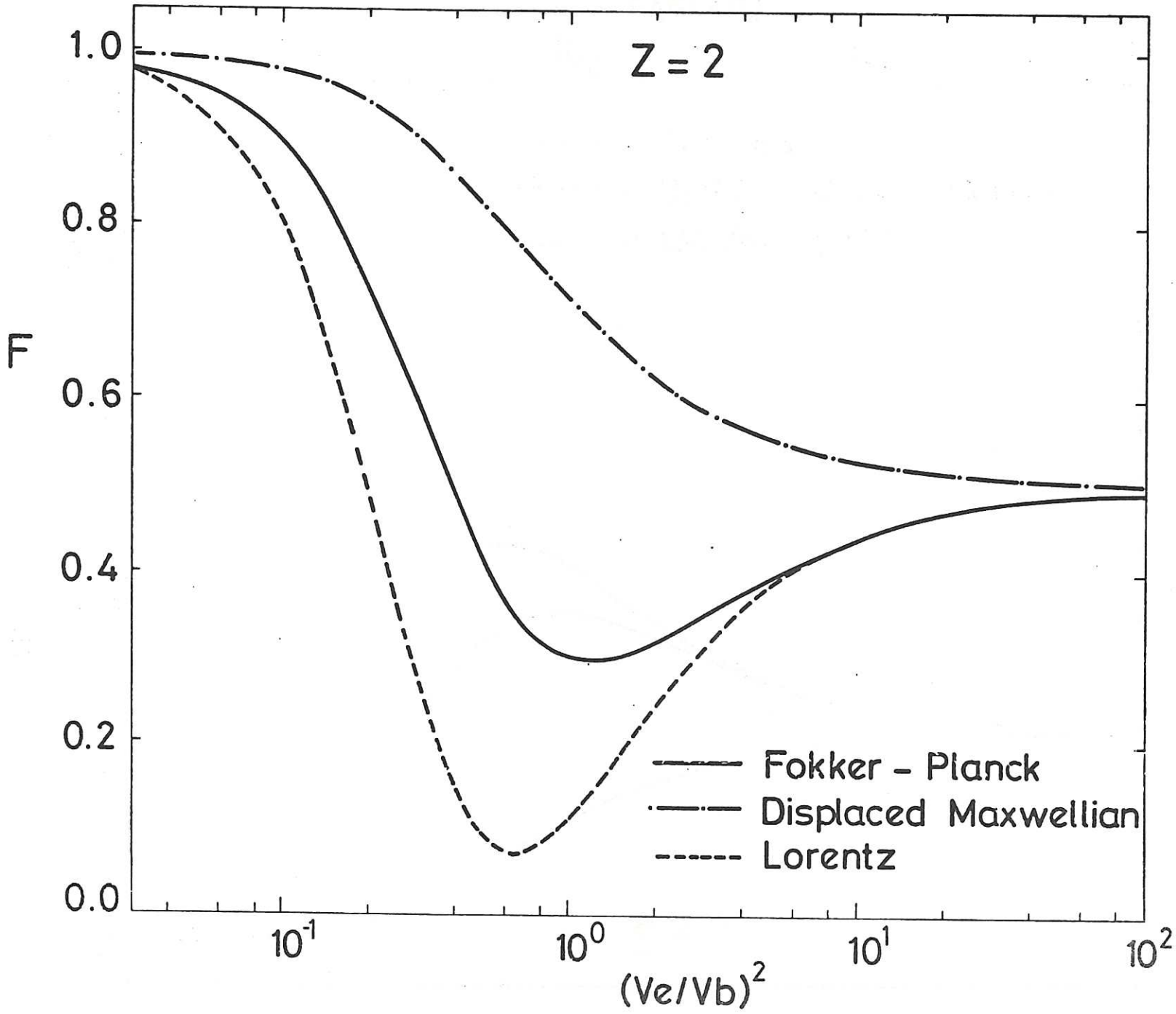
Z = 2
F
1.0
0.8
0.6
0.4
0.2
0.0
10^{-1}
10^{0}
10^{1}
10^{2}
$(Ve/Vb)^2$
Fokker - Planck
Displaced Maxwellian
Lorentz

FIG 2

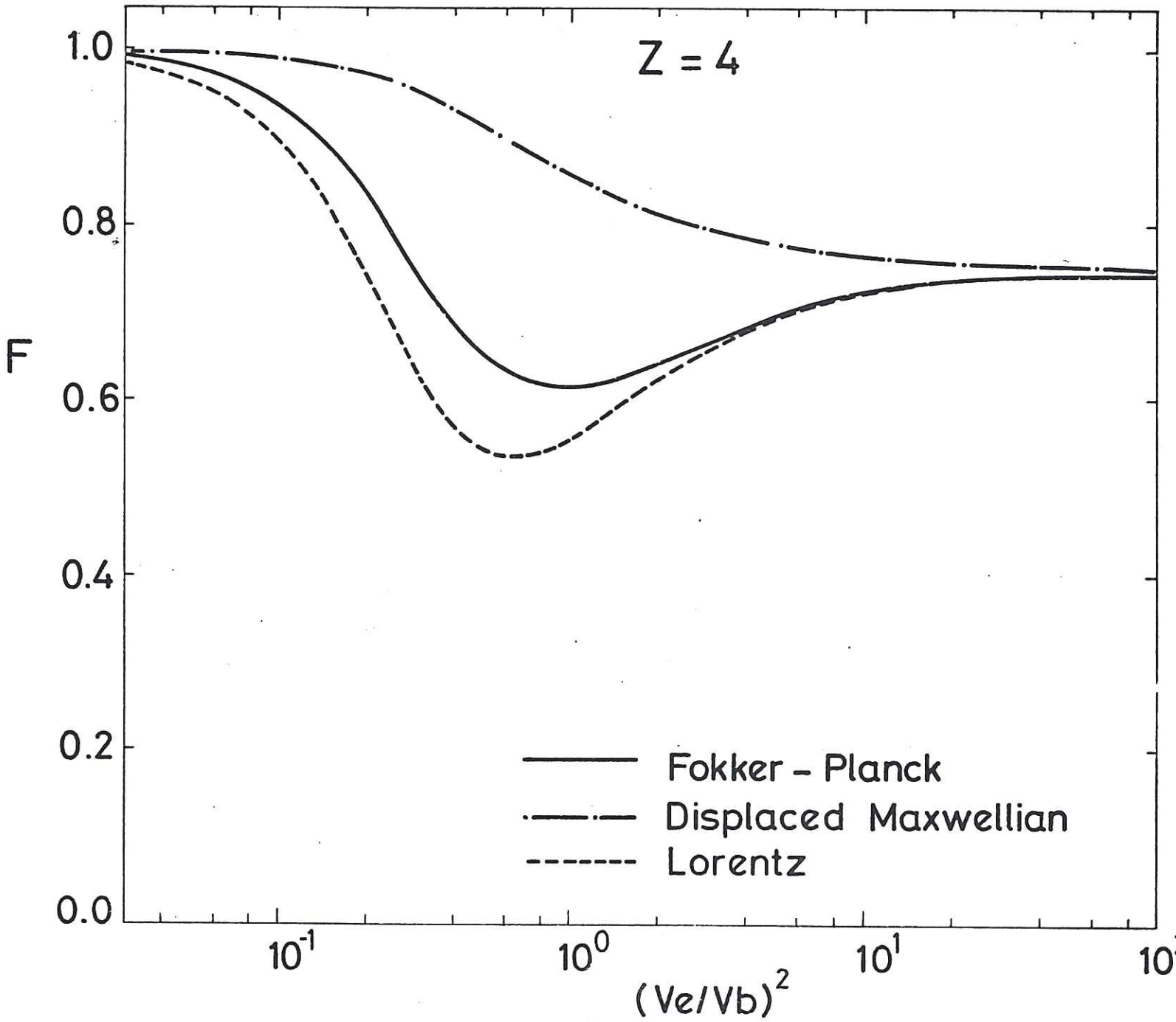
Z = 4
F
1.0
0.8
0.6
0.4
0.2
0.0
10^{-1}
10^{0}
10^{1}
10^{2}
$(Ve/Vb)^2$
Fokker – Planck
Displaced Maxwellian
Lorentz

FIG 3

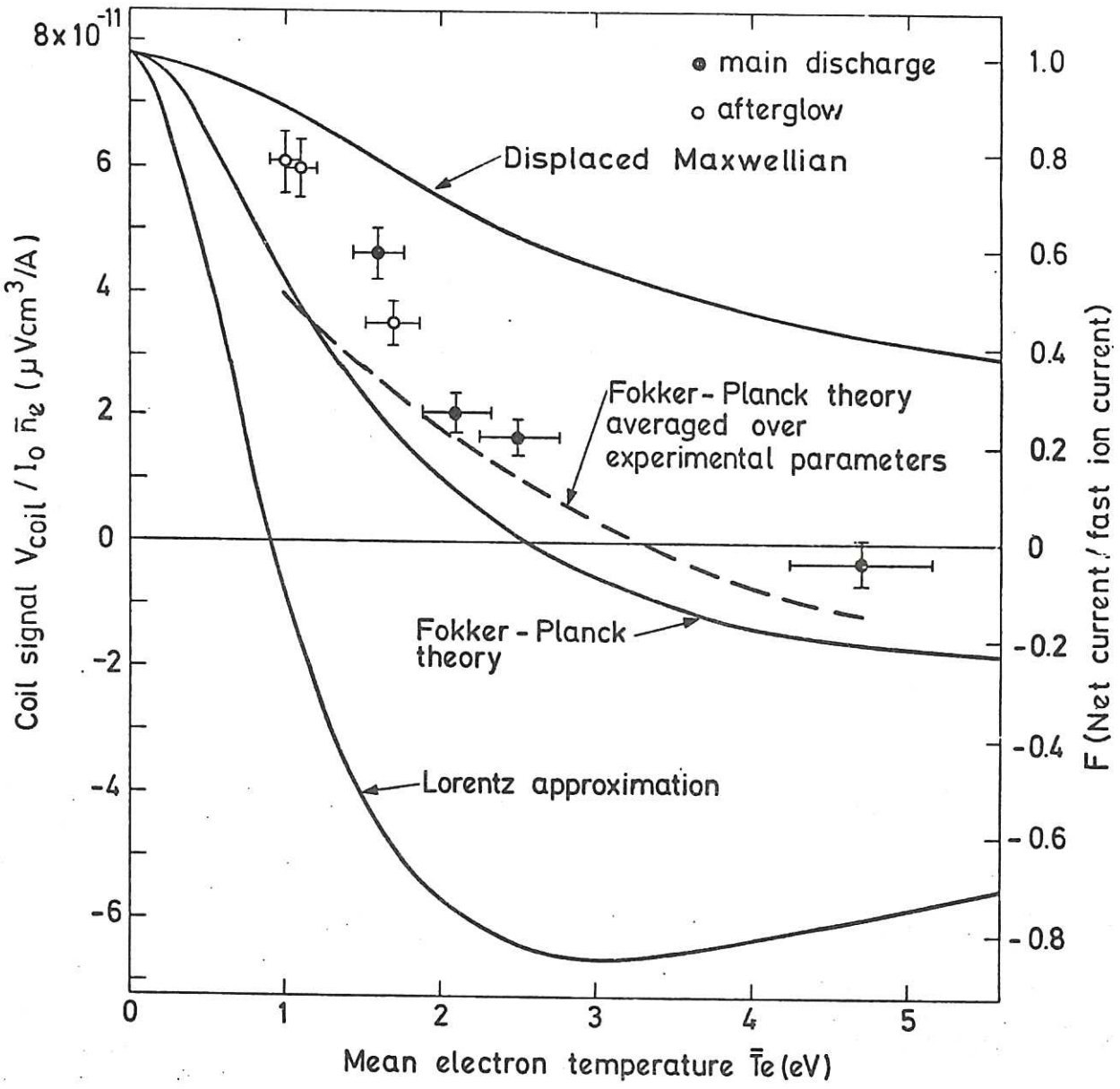
8x10^-11
6
4
2
0
-2
-4
-6
1.0
0.8
0.6
0.4
0.2
0
-0.2
-0.4
-0.6
-0.8
0
1
2
3
4
5
main discharge
afterglow
Displaced Maxwellian
Fokker-Planck theory averaged over experimental parameters
Fokker-Planck theory
Lorentz approximation
Coil signal Vcoil / Io ñe (μVcm3/A)
F (Net current / fast ion current)
Mean electron temperature Te (eV)

FIG 4